

**Synchronizing the
Greenland ice core
and radiocarbon
timescales**

F. Adolphi and
R. Muscheler

Synchronizing the Greenland ice core and radiocarbon timescales over the Holocene – Bayesian wiggle-matching of cosmogenic radionuclide records

F. Adolphi and R. Muscheler

Department of Geology – Quaternary Science, Lund University, Sweden

Received: 16 June 2015 – Accepted: 19 June 2015 – Published: 09 July 2015

Correspondence to: F. Adolphi (florian.adolphi@geol.lu.se)

Published by Copernicus Publications on behalf of the European Geosciences Union.

Title Page

Abstract

Introduction

Conclusions

References

Tables

Figures

◀

▶

◀

▶

Back

Close

Full Screen / Esc

Printer-friendly Version

Interactive Discussion

Abstract

Investigations of past climate dynamics rely on accurate and precise chronologies of the employed climate reconstructions. The radiocarbon dating calibration curve (IntCal13) and the Greenland ice core chronology (GICC05) represent two of the most widely used chronological frameworks in paleoclimatology of the past ~ 50 000 years. However, comparisons of climate records anchored on these chronologies are hampered by the precision and accuracy of both timescales. Here we use common variations in the production rates of ^{14}C and ^{10}Be recorded in tree-rings and ice cores, respectively, to assess the differences between both timescales during the Holocene. We employ a novel statistical approach which leads to strongly reduced and yet, more robust, uncertainty estimates in comparison to earlier work. We demonstrate that the inferred timescale differences are robust independent of (i) the applied ice core ^{10}Be records, (ii) assumptions of the mode of ^{10}Be deposition, as well as (iii) carbon cycle effects on ^{14}C , and in agreement with independent estimates of the timescale differences. Our results imply that the GICC05 counting error is likely underestimated during the most recent 2000 years leading to a dating bias that propagates throughout large parts of the Holocene. Nevertheless, our analysis indicates that the GICC05 counting error is generally a robust uncertainty measurement but care has to be taken when treating it as a nearly Gaussian error distribution. The proposed IntCal13-GICC05 transfer function facilitates the comparison of ice core and radiocarbon dated paleoclimate records at high chronological precision.

1 Introduction

Paleoclimatology can provide significant insights into natural climate changes and thus, improve our understanding of the climate system. Besides the reconstruction of past climate itself, a precise chronology of each paleoclimate record is crucial to reliably assess the dynamics of the inferred changes. Furthermore, consistent chronologies

CPD

11, 2933–2975, 2015

Synchronizing the Greenland ice core and radiocarbon timescales

F. Adolphi and
R. Muscheler

Title Page

Abstract

Introduction

Conclusions

References

Tables

Figures

◀

▶

◀

▶

Back

Close

Full Screen / Esc

Printer-friendly Version

Interactive Discussion

Synchronizing the Greenland ice core and radiocarbon timescales

F. Adolphi and
R. Muscheler

Title Page

Abstract

Introduction

Conclusions

References

Tables

Figures

◀

▶

◀

▶

Back

Close

Full Screen / Esc

Printer-friendly Version

Interactive Discussion

across multiple paleoclimate records are required to assess the spatiotemporal evolution of climatic events and thus, to test for potential leads and lags within the climate system and ultimately improve the understanding of the underlying processes of past climate change. Two independent key timescales in paleoclimatology of the past 50 000 years are the radiocarbon- (IntCal13, Reimer et al., 2013) and the Greenland ice core timescale (GICC05, Andersen et al., 2006; Rasmussen et al., 2006; Seierstad et al., 2014; Svensson et al., 2008; Vinther et al., 2006). To be able to infer leads and lags between paleoclimatic changes anchored on these chronologies at high precision, it is crucial to test the consistency of both timescales and establish climate-independent isochrones and thus, reduce the influence of their absolute dating uncertainties (e.g., Lane et al., 2013). One method to compare and synchronize both timescales is the use of cosmogenic radionuclide records, such as ^{10}Be and ^{14}C (Muscheler et al., 2014a, b; Muscheler et al., 2008; Southon, 2002).

Cosmogenic radionuclides such as ^{10}Be and ^{14}C are produced in the atmosphere through a nuclear cascade mainly triggered by incoming galactic cosmic rays (gcr, Lal and Peters, 1967). The flux of gcr reaching the atmosphere is in turn modulated by the strength of the helio- and geo-magnetic fields resulting in varying production rates of ^{10}Be and ^{14}C (Masarik and Beer, 2009, 1999; Kovaltsov et al., 2012; Kovaltsov and Usoskin, 2010). Thus, increased (decreased) intensity of the solar- and/or geomagnetic field will result in decreased (increased) cosmogenic radionuclide production rates. Therefore, ^{14}C and ^{10}Be production rates co-vary globally due to external processes, making them an ideal synchronization tool.

After production ^{14}C oxidizes to $^{14}\text{CO}_2$ that enters the global carbon cycle and gets stored in various environmental archives such as tree-rings, sediments, and speleothems. ^{10}Be attaches to aerosols which are deposited within 1–2 years (Raisbeck et al., 1981) by wet and dry deposition processes and stored in sediments including polar ice sheets. These “system effects” (i.e., non-production influences on ^{10}Be and ^{14}C records such as the mixing, transport, and deposition of ^{14}C and ^{10}Be) can challenge an unequivocal reconstruction of cosmogenic radionuclide production rates

has the advantage that it can provide continuous estimates of time scale differences as opposed to discrete tie-points obtained from tephrochronology (Abbott and Davies, 2012; Lane et al., 2013) or changes in atmospheric trace gases (Blunier et al., 1998; Buizert et al., 2015).

1.1 Aim of this study

Recently, Muscheler et al. (2014a) assessed the differences of the radiocarbon and ice core time scales for the past 14 000 years by comparing GRIP ^{10}Be (Yiou et al., 1997; Muscheler et al., 2004b; Vonmoos et al., 2006) and IntCal13 ^{14}C data (Reimer et al., 2013). Here, we revisit this approach using a different statistical framework (Bronk Ramsey et al., 2001) that is computationally less expensive and provides improved error estimates for the inferred timescale differences as compared to the method used in Muscheler et al. (2014a). Furthermore, we test the robustness of the obtained results with respect to the use of different ice core ^{10}Be records as well as potential “system effects” on the radionuclide records. We focus our analysis on the period where dendrochronologically dated high quality ^{14}C measurements on tree-rings are available. While this is theoretically the case back to 12 560 calBP (calibrated before present, AD1950, Friedrich et al., 2004), the accuracy of the oldest part of tree-ring chronology has recently been questioned (Hogg et al., 2013) causing a gap in the ^{14}C records underlying IntCal13 around 12 000 calBP (Reimer et al., 2013). Hence, we limit our analysis to the Holocene where both dendrochronological and ^{14}C -data replication is high and most robust (Reimer et al., 2013; Friedrich et al., 2004).

2 Methods

2.1 Data

The key data used in this paper is shown in Fig. 1. The GRIP ^{10}Be record (Vonmoos et al., 2006; Muscheler et al., 2004b; Yiou et al., 1997) covers almost the entire

Synchronizing the Greenland ice core and radiocarbon timescales

F. Adolphi and
R. Muscheler

Title Page

Abstract

Introduction

Conclusions

References

Tables

Figures

◀

▶

◀

▶

Back

Close

Full Screen / Esc

Printer-friendly Version

Interactive Discussion



$\Delta^{14}\text{C}$ anomalies ($R_{i;n}$) for which we know the absolute age differences (Δt_i) between each sample from ice core layer counting. We can estimate the probability (P_i) for different assumed time scale differences between the records (t_s) for each sample by using Eq. (8) in Bonk Ramsey et al. (2001):

$$P_i(t_s + \Delta t_i) \propto \frac{\exp\left(-\frac{(R_i - R(t_s + \Delta t_i))^2}{2(\delta R_i^2 + \delta R^2(t_s + \Delta t_i))}\right)}{\sqrt{\delta R_i^2 + \delta R^2(t_s + \Delta t_i)}} \quad (1)$$

Using Bayes' theorem to combine the probabilities for each individual measurement we can obtain an overall probability (P_s) for each time scale difference between GICC05 and IntCal13 (Eq. 9 in Bonk Ramsey et al., 2001):

$$P_s(t_s) \propto \prod_{i=1}^n P_i(t_s + \Delta t_i) \quad (2)$$

To allow a continuous comparison, all records have been interpolated to annual resolution. However, since the ice core sampling resolution is in reality lower we do not obtain truly independent probability distributions for each sample. Consequently, we correct for the reduced degrees of freedom by scaling P_s as:

$$P_{s_{\text{scaled}}}(t_s) = P_s(t_s)^{1/r} \quad (3)$$

where r is the original sample spacing (years/sample) of the ice core ^{10}Be records. This scaling effectively widens the obtained probability distribution and thus, increases the derived uncertainties. For the filtered GRIP ^{10}Be record, we assume a decadal resolution.

This “wobble-matching” is done for predefined windows of IntCal13 and GRIP and hence, yields a probability distribution ($P_{s_{\text{scaled}}}(t_s)$) for their time scale difference for each

Synchronizing the Greenland ice core and radiocarbon timescales

F. Adolphi and
R. Muscheler

Title Page

Abstract

Introduction

Conclusions

References

Tables

Figures

◀

▶

◀

▶

Back

Close

Full Screen / Esc

Printer-friendly Version

Interactive Discussion



then maintained for 25 000 years to reach equilibrium again (steady state) before linearly changing the perturbed parameter back to preindustrial values within 50 years (transition 2). We use these different sensitivity experiments to obtain an uncertainty estimate of the modelled (^{10}Be -based) $\Delta^{14}\text{C}$ records due to carbon cycle effects.

2.4.2 $^{10}\text{Be}/^{14}\text{C}$ production rate ratio

To compare tree-ring and ice core radionuclide records we used the normalized ^{10}Be records as ^{14}C production rate input for the carbon cycle model. This yields a ^{10}Be -based $\Delta^{14}\text{C}$ anomaly record that can be directly compared to the tree-ring data. Hence, we have to assume a ratio between the production rates of ^{14}C and ^{10}Be . This ratio depends on the radionuclide production cross-sections and the energy spectrum of the incoming gcr. Model estimates of relative $^{14}\text{C} : ^{10}\text{Be}$ production rate increases for a change in the solar modulation parameter from 700 to 0 MeV at modern geomagnetic field strength differ between 1.34 (Masarik and Beer, 2009) and 1.04 (Kovaltsov et al., 2012; Kovaltsov and Usoskin, 2010). Similarly, the predicted $^{14}\text{C} : ^{10}\text{Be}$ production rate ratios for changes in the geomagnetic field strength are model dependent for unresolved reasons (Cauquoin, 2014).

Furthermore, the $^{14}\text{C} : ^{10}\text{Be}$ production rate ratio depends on the presence of a potential “polar bias” (see Sect. 1). If a “polar bias” was present (Bard et al., 1997; Field et al., 2006) the ratio between ^{14}C and ice core ^{10}Be variations could be biased towards lower values (Bard et al. (1997) report a value of 0.65 for the South Pole ^{10}Be record). For Greenland, however, high resolution ^{10}Be records do not support such a strong polar bias but would instead be consistent with a well-mixed atmosphere (Pedro et al., 2012; Muscheler and Heikkilä, 2011). Simply comparing the standard deviations of centennial variations of IntCal13 and ^{10}Be -based $\Delta^{14}\text{C}$ anomalies leads to ratios between 0.95 and 1.05 ($\sigma^{14}\text{C}_{\text{IntCal}}/\sigma^{14}\text{C}_{^{10}\text{Be}}$) depending on which ice core (GRIP/GISP2) and which version of the ^{10}Be records (concentration, flux, climate corrections) is used. Thus, we start with a $^{14}\text{C} : ^{10}\text{Be}$ production rate ratio of 1 : 1 and test the sensitivity of

Synchronizing the Greenland ice core and radiocarbon timescales

F. Adolphi and
R. Muscheler

Title Page

Abstract

Introduction

Conclusions

References

Tables

Figures

◀

▶

◀

▶

Back

Close

Full Screen / Esc

Printer-friendly Version

Interactive Discussion



our results to this assumption by repeating the calculations outlined in Sect. 2.2 using $^{14}\text{C} : ^{10}\text{Be}$ ratios of 1.5 : 1 and 0.5 : 1.

2.5 Timescale transfer function

The methodology outlined in Sect. 2.2 yields a probability estimate of the IntCal13-GICC05 timescale difference every 50 years. These probability distributions are however not fully independent since neighbouring 1000 year windows overlap and are, hence, largely based on the same data. To create a timescale transfer-function we employed a Monte-Carlo procedure that creates 20 000 possible transfer functions based on independent, i.e. non-overlapping, windows. Each iteration, (i) randomly selects one of the youngest (most recent) 20 windows and (ii) randomly samples from the probability distribution $P_{\text{scaled}}(t_s)$ of this window as well as the older non-overlapping windows (i.e. one window every 1000 years so that the selected windows are fully independent with respect to the data points they contain). The resulting transfer functions are then interpolated to annual resolution and converted into probability distributions for the timescale difference at each point in time. For each transfer function we assume that both timescales are correct at 0 BP (i.e. AD 1950).

2.6 Iterative structure of the synchronization method

The separate aspects of our synchronization method outlined above are applied in an iterative manner to obtain robust and self-consistent error estimates for our results. The different steps involved are carried out in the following order:

1. We create four versions of both ice core ^{10}Be records as endmembers of plausible ^{10}Be production rate histories (see Sect. 2.3).
2. We convert these ^{10}Be records into $\Delta^{14}\text{C}$ using a box-diffusion carbon cycle model (Sect. 2.4.1) assuming a $^{14}\text{C} : ^{10}\text{Be}$ production rate ratio of 1 (see Sect. 2.4.2).

Synchronizing the Greenland ice core and radiocarbon timescales

F. Adolphi and
R. Muscheler

Title Page

Abstract

Introduction

Conclusions

References

Tables

Figures

◀

▶

◀

▶

Back

Close

Full Screen / Esc

Printer-friendly Version

Interactive Discussion



Synchronizing the Greenland ice core and radiocarbon timescales

F. Adolphi and
R. Muscheler

3. The difference between the different ^{10}Be -based $\Delta^{14}\text{C}$ records, and results from the carbon cycle sensitivity experiments (see Sect. 2.4.1) serve as initial uncertainty estimates for the ^{10}Be -based $\Delta^{14}\text{C}$ records.
4. We then compare the tree-ring and ^{10}Be -based $\Delta^{14}\text{C}$ records with respect to their timescale differences using the statistics outlined in Sect. 2.2. We test for the robustness of these results by using all four different ^{10}Be versions of both GRIP and GISP2 separately as well as ^{10}Be - ^{14}C conversion factors of 0.5 and 1.5 (see Sect. 2.4.2).
5. Calculating an initial timescale transfer-function (see Sect. 2.5) we then synchronize IntCal13 and GICC05. This enables us to directly compare tree-ring and ^{10}Be -based $\Delta^{14}\text{C}$ records and estimate the optimal $^{14}\text{C} : ^{10}\text{Be}$ production rate ratio, as well as uncertainties for the ^{10}Be -based $\Delta^{14}\text{C}$ record.
6. Based on these posterior estimates of the $^{14}\text{C} : ^{10}\text{Be}$ ratio and the uncertainty of the ^{10}Be records, we repeat the calculations outlined in Sects. 2.2 and 2.5 yielding our final estimates of the IntCal13-GICC05 timescale differences over the Holocene.

3 Results

3.1 Climate and Carbon cycle related uncertainties in the GRIP and GISP2 ^{10}Be records

Figure 2 displays the different ^{10}Be production rate scenarios from GRIP (top two panels) and GISP2 (lower two panels) ^{10}Be concentrations (Conc), fluxes (Flux) and their climate corrected versions (Conc_{clim} and Flux_{clim}, respectively). Dividing the ^{10}Be records into a centennial (< 500 years) and millennial (> 500 years) variations indicates that the different ^{10}Be versions mainly differ in the low frequency range. These millennial differences can systematically affect the modelling of $\Delta^{14}\text{C}$ since the carbon cycle

[Title Page](#)[Abstract](#)[Introduction](#)[Conclusions](#)[References](#)[Tables](#)[Figures](#)[◀](#)[▶](#)[◀](#)[▶](#)[Back](#)[Close](#)[Full Screen / Esc](#)[Printer-friendly Version](#)[Interactive Discussion](#)

Synchronizing the Greenland ice core and radiocarbon timescales

F. Adolphi and
R. Muscheler

Title Page

Abstract

Introduction

Conclusions

References

Tables

Figures

◀

▶

◀

▶

Back

Close

Full Screen / Esc

Printer-friendly Version

Interactive Discussion

about $\pm 3\%$ (Fig. 4d) except for about 200–300 years around the timing of the carbon cycle perturbation itself (Fig. 4, transitions 1 and 2). Importantly, the phase of the centennial $\Delta^{14}\text{C}$ variations is not affected by the imposed carbon cycle changes. Since the applied carbon cycle changes in our sensitivity experiments are likely unrealistically large for Holocene conditions (Köhler et al., 2006; Roth and Joos, 2013), we conservatively assume a 1σ uncertainty of $\pm 3\%$ (see Fig. 4d, “steady state”) for the modelled $\Delta^{14}\text{C}$ records due to carbon cycle effects.

Adding the uncertainties due to climate impacts on ^{10}Be ($\pm 3\%$) and the carbon cycle ($\pm 3\%$) in quadrature we thus, obtain an initial uncertainty estimate of about $\pm 4.5\%$ for the modelled $\Delta^{14}\text{C}$ records.

3.2 Sensitivity of the synchronization method to uncertainties in the ^{10}Be - ^{14}C conversion

In the following we will compare the centennial $\Delta^{14}\text{C}$ anomalies reconstructed from tree-rings (IntCal13) and ice cores (GRIP/GISP2 ^{10}Be -based) with respect to their timescale differences. We use the statistical framework outlined in Sect. 2.2 and assign an initial uncertainty of $\pm 4.5\%$ to the ^{10}Be -based $\Delta^{14}\text{C}$ records. The uncertainties for the tree-ring based $\Delta^{14}\text{C}$ anomalies are taken from IntCal13 (Reimer et al., 2013). For this purpose we spliced the GISP2 ^{10}Be versions into the corresponding GRIP ^{10}Be versions to fill the gap in the GRIP record between 9400 and 10 800 years BP to create a continuous record for the entire Holocene. Hence, in the following “GRIP” refers to this combination of GRIP and GISP2 data, while results for the GISP2 data are only shown for periods where they have not been used to fill the gap in the GRIP record.

Figure 5 displays the obtained probability distributions $P_{S_{\text{scaled}}}(t_s)$ for each sliding window, centred on its mean age. The results are shown for all four GRIP ^{10}Be versions (Fig. 5a), in comparison to results based on GISP2 data only (Fig. 5b), as well as for different assumed $^{14}\text{C} : ^{10}\text{Be}$ production rate ratios (Fig. 5c). The different GRIP ^{10}Be versions yield consistent estimates of the IntCal13-GICC05 timescale differences

Synchronizing the Greenland ice core and radiocarbon timescales

F. Adolphi and
R. Muscheler

Title Page

Abstract

Introduction

Conclusions

References

Tables

Figures

◀

▶

◀

▶

Back

Close

Full Screen / Esc

Printer-friendly Version

Interactive Discussion

throughout the Holocene. The only marked difference occurs around the 8.2 kaBP event (Blockley et al., 2012). During this period the ^{10}Be flux indicates a more rapid increase in the IntCal13-GICC05 timescale difference as compared to all other ^{10}Be versions. As noted by Muscheler et al. (2004a) the accumulation rate anomaly associated to the climate oscillation around 8200 year ago appears to lead to an “over-correction” of the ^{10}Be deposition during flux calculation. This leads to a worse agreement between ^{14}C and ^{10}Be -fluxes as compared to ^{14}C and ^{10}Be concentrations (see Fig. 3 in Muscheler et al., 2004a). This is corroborated by the fact that results based on the “climate corrected” ^{10}Be flux follow the probability estimates of ^{10}Be concentrations (Fig. 5a).

Comparing GRIP based results to GISP2 based estimates indicates consistent estimates of the timescale differences. The larger uncertainties of the GISP2 based results are due to the lower sampling resolution of the GISP2 ^{10}Be record (see Eq. 3).

Figure 5c shows the sensitivity of our results to the assumed $^{14}\text{C} : ^{10}\text{Be}$ production-rate ratio. It can be seen that the inferred timescale differences are relatively insensitive to the assumed $^{14}\text{C} : ^{10}\text{Be}$ ratio. However, the derived uncertainty of $P_{\text{scaled}}(t_s)$ does increase with lower $^{14}\text{C} : ^{10}\text{Be}$ ratios. This can easily be understood by imagining a scaling of zero for the ^{10}Be -based record which would result in an infinitely wide probability distribution.

In summary, our method of estimating the IntCal13-GICC05 timescale difference is (i) largely robust for all versions of the GRIP ^{10}Be record, (ii) consistent for GRIP and GISP2 ^{10}Be data, and (iii) independent of the assumed $^{14}\text{C} : ^{10}\text{Be}$ production-rate ratio. However, this analysis also shows that it is important to compare ^{10}Be concentrations and fluxes to identify potential caveats as seen around the 8.2 kaBP event. Furthermore, while the estimate of the most likely timescale difference (i.e. the location of the maximum of $P_{\text{scaled}}(t_s)$) may not be affected by the assumed $^{14}\text{C} : ^{10}\text{Be}$ ratio, the uncertainty of this estimate is. Hence, in the following section we will derive a posterior estimate of the $^{14}\text{C} : ^{10}\text{Be}$ ratio, as well as a refined uncertainty estimate of the ^{10}Be -based $\Delta^{14}\text{C}$ records.

3.3 Posterior estimate of the $^{14}\text{C} : ^{10}\text{Be}$ production rate ratios and uncertainties

As shown in the previous section, our estimates of the most likely timescale difference between IntCal13 and GICC05 are largely independent of which ^{10}Be record (GRIP/GISP2) and which version thereof (concentration, flux, climate corrections) is used, as well as which $^{14}\text{C} : ^{10}\text{Be}$ ratio is assumed. Hence, we calculated an initial GICC05-IntCal13 transfer function (Sect. 2.5) and synchronized the tree-ring based and ^{10}Be -based $\Delta^{14}\text{C}$ record. This enables us to compare both records with respect to the most likely $^{14}\text{C} : ^{10}\text{Be}$ ratio. In addition, we can compare both records to derive a posterior estimate of the modelled ^{10}Be -based $\Delta^{14}\text{C}$ uncertainty.

After synchronization we can compare tree-ring and ^{10}Be -based $\Delta^{14}\text{C}$ sample pairs assuming different ^{10}Be scaling factors (i.e. $^{14}\text{C} : ^{10}\text{Be}$ ratios) between zero and two. The difference between tree-ring and ^{10}Be -based $\Delta^{14}\text{C}$ sample pairs ($\delta(t)$) is a function of the uncertainty of IntCal13 ($\delta_{\text{IC}}(t)$) and the uncertainty of the ^{10}Be -based records ($\delta_{\text{Be}}(t)$) in the form that:

$$\delta(t) = \sqrt{\delta(t)_{\text{IC}}^2 + \delta(t)_{\text{Be}}^2} \quad (4)$$

Hence, we can rearrange Eq. (4) and use the quoted uncertainties of IntCal13 to derive $\delta_{\text{Be}}(t)$. These uncertainties can be summarized to the rooted mean square error (RMSE $_{^{10}\text{Be}}$). This way we can obtain the optimal ^{10}Be scaling factor (where the RMSE $_{^{10}\text{Be}}$ minimizes) and the associated uncertainty of the ^{10}Be -based $\Delta^{14}\text{C}$ records (the minimum of the RMSE $_{^{10}\text{Be}}$). Figure 6 displays the results of this analysis indicating an optimal ^{10}Be scaling-factor of around 0.7. This would imply a strong polar bias of the GRIP and GISP2 ^{10}Be records. However, when investigating the $\Delta^{14}\text{C}$ time series it becomes apparent, that this low scaling leads to an underestimation of the amplitude of virtually all grand solar maxima and minima (i.e. large $\Delta^{14}\text{C}$ anomalies) in the ^{10}Be -based $\Delta^{14}\text{C}$ record (Fig. 7, top). This bias is induced by the fact, that the $\Delta^{14}\text{C}$ anomalies are normally distributed around 0‰ leading to a majority of the $\Delta^{14}\text{C}$ values

lying close to zero dominating the $\text{RMSE}_{10\text{Be}}$. Hence, for these values a low scaling of the ^{10}Be -based $\Delta^{14}\text{C}$ records will simply act to reduce noise from the record and thus, reduce the $\text{RMSE}_{10\text{Be}}$.

To avoid this bias, we performed a binned regression analysis. We divided the tree-ring and ^{10}Be -based $\Delta^{14}\text{C}$ sample pairs into bins of 2.5 ‰ (defined based on the tree-ring $\Delta^{14}\text{C}$ anomalies) and calculated the $\text{RMSE}_{10\text{Be}}$ for each bin ($\text{RMSE}_{10\text{Be_bin}}$). These uncertainties for each bin can then be summarized to an overall $\text{RMSE}_{10\text{Be}}$ as:

$$\text{RMSE}_{10\text{Be}} = \sqrt{\text{RMSE}_{10\text{Be_bin}}^2} \quad (5)$$

This binning leads to an equal weighting of small and large $\Delta^{14}\text{C}$ anomalies in the comparison of the $\Delta^{14}\text{C}$ records. It can be seen that this method indicates a larger $^{14}\text{C} : ^{10}\text{Be}$ ratio of about 1.1 (Fig. 8) and avoids the systematic underestimation of large amplitude $\Delta^{14}\text{C}$ anomalies (Fig. 7, bottom). Depending on the production rate model used, this scaling indicates a weak (Masarik and Beer, 2009, 1999) or no (Kovaltsov et al., 2012; Kovaltsov and Usoskin, 2010) polar bias in the Greenland ^{10}Be records. In addition, it can be seen that the minimum of the $\text{RMSE}_{10\text{Be}}$ becomes larger than without binning indicating an uncertainty of about 4 ‰ for the ^{10}Be -based $\Delta^{14}\text{C}$ records. This is due to the above described effect, that the noise is not artificially suppressed and can be seen by comparing the decadal scale peaks in the top and bottom panels of Fig. 7. The larger ^{10}Be scaling factor makes the ^{10}Be record appear noisier. However, firstly, this noise may represent remaining influences of “system effects” on ice core ^{10}Be records and hence, represent an uncertainty that has to be taken into account. Secondly, it should be kept in mind that IntCal13 is a stack of multiple ^{14}C datasets which will inevitably result in smoothing. This smoothing may also reduce the amplitude of “real” $\Delta^{14}\text{C}$ variations instead of merely reducing noise, since the differences between the underlying raw-data sets of IntCal13 are potentially in part systematic (Stuiver et al., 1998; Adolphi et al., 2013).

Synchronizing the Greenland ice core and radiocarbon timescales

F. Adolphi and
R. Muscheler

[Title Page](#)[Abstract](#)[Introduction](#)[Conclusions](#)[References](#)[Tables](#)[Figures](#)[◀](#)[▶](#)[◀](#)[▶](#)[Back](#)[Close](#)[Full Screen / Esc](#)[Printer-friendly Version](#)[Interactive Discussion](#)

In conclusion we use a $^{14}\text{C} : ^{10}\text{Be}$ ratio of 1.1 : 1 and an uncertainty of 4‰ for the modelled $\Delta^{14}\text{C}$ record to derive a final IntCal13-GICC05 transfer function in the next section.

3.4 IntCal13-GICC05 transfer function

Using the estimated $^{14}\text{C} : ^{10}\text{Be}$ ratio of 1.1 and a ^{10}Be -based $\Delta^{14}\text{C}$ error of $\pm 4\%$ ($\pm 1\sigma$) (see previous section) we recalculated the “wiggle-match” probability distributions ($P_{\text{scaled}}(t_s)$, Eq. 3) for the IntCal13-GICC05 timescale difference (Fig. 9, grey shading). For these calculations we used the mean of all GRIP ^{10}Be -based $\Delta^{14}\text{C}$ versions (concentration, flux, climate corrections) and filled the gap between 9400 and 10800 yearsBP using the GISP2 data. Based on these probability distributions we modelled the IntCal13-GICC05 transfer function as described in Sect. 2.5. The resulting transfer function (Fig. 9 solid lines) averages out some short-term fluctuations in the timescale difference compared to the initial “wiggle-match” probability distributions. As described in Sect. 2.5 this is due to the used window length of 1000 years to determine $P_{\text{scaled}}(t_s)$ at each point in time, preventing an independent assessment of faster changes in the timescale difference. Nevertheless, the estimated uncertainties of the timescale transfer-function (thin black lines in Fig. 9) encompass the uncertainties of the “wiggle-match” probability distribution at each point in time.

4 Discussion

Figure 10 shows the obtained estimate of the IntCal13-GICC05 timescale difference in comparison to the results obtained by using the method of Muscheler et al. (2014a, re-run with a 1000 year window length) and age markers that have been independently anchored on both timescales.

Our results are fully consistent with the results obtained by Muscheler et al. (2014a). While this is expected to some extent, as both our study and the work by Muscheler

Synchronizing the Greenland ice core and radiocarbon timescales

F. Adolphi and
R. Muscheler

Title Page

Abstract

Introduction

Conclusions

References

Tables

Figures

◀

▶

◀

▶

Back

Close

Full Screen / Esc

Printer-friendly Version

Interactive Discussion



Synchronizing the Greenland ice core and radiocarbon timescales

F. Adolphi and
R. Muscheler

et al. (2014a) are based on the same data, it shows that the statistical approach used here leads to similar results as the Monte-Carlo lag-correlation analysis but is computationally much less expensive. Furthermore, as shown in Fig. 5, we obtain similar results when using the GISP2 ^{10}Be instead of the GRIP ^{10}Be record lending additional support to the robustness of our results. The additional modelling of the transfer function employed here (Sects. 2.5 and 3.4) leads to a smoother development of the timescale difference which is more realistically reflecting limitations of the method imposed by the window size of the ^{14}C - ^{10}Be comparison. The difference between both timescale transfer-functions around 8200 years BP is induced by the fact that Muscheler et al. (2014a) based their calculations on ^{10}Be fluxes which are influenced by accumulation rate changes around this time as discussed in Sect. 3.2 and in Muscheler et al. (2004a).

The largest difference between the results presented here and by those of Muscheler et al. (2014a) is seen in the derived error estimates. We obtain strongly reduced uncertainties for the estimated timescale differences. This is likely due to the fact, that Muscheler et al. (2014a) used a comparably ad-hoc and highly conservative method to derive their uncertainties. By taking the distribution of the mean r^2 values of all iterations Muscheler et al. (2014a) do not include the results of the Monte-Carlo analysis of the “Best-Fits” in their error estimate. Thus, ^{14}C - ^{10}Be matches that may not be the most likely solution in any of the iterations become included in the uncertainty envelope. In comparison, the statistics employed here allow a direct analytical assessment of the synchronization uncertainties. Hence, while our uncertainty estimates are significantly smaller, we consider them more robust. Theoretically, systematic errors from undetected biases in the ^{10}Be record could lead to erroneous results. However, the results shown in Sect. 3.2 demonstrate the consistency of GRIP and GISP2 ^{10}Be -based calculations as well as for different climate corrections and do, thus, not indicate such biases (see Fig. 5). In conclusion, while largely consistent, we regard the method employed here a significant improvement to the approach by Muscheler et al. (2014a).

[Title Page](#)[Abstract](#)[Introduction](#)[Conclusions](#)[References](#)[Tables](#)[Figures](#)[◀](#)[▶](#)[◀](#)[▶](#)[Back](#)[Close](#)[Full Screen / Esc](#)[Printer-friendly Version](#)[Interactive Discussion](#)

Synchronizing the Greenland ice core and radiocarbon timescales

F. Adolphi and
R. Muscheler

Title Page

Abstract

Introduction

Conclusions

References

Tables

Figures

◀

▶

◀

▶

Back

Close

Full Screen / Esc

Printer-friendly Version

Interactive Discussion

Comparing our results to independent estimates of IntCal13-GICC05 timescale differences further supports our analyses (Fig. 10, symbols). Two major solar proton events (“775 and 994 AD events”) leaving well-defined spikes in the ^{14}C content of dendrochronologically dated trees (Miyake et al., 2013, 2012; Gütler et al., 2015) as well as in Greenland ice core ^{10}Be records (Mekhaldi et al., 2015; Sigl et al., 2015) indicate an IntCal13-GICC05 timescale difference of -7 ± 2 years (2σ) for both events (Sigl et al., 2015). Consistent with these findings, we obtain IntCal13-GICC05 differences of -4 ± 4 and -6 ± 5 years (2σ) for the 994 and 775 AD event, respectively. It should be noted that these annual radionuclide excursions are not present in the data used here, which are of lower resolution, and are hence, independent estimates of the timescale difference.

Based on tephra findings in the GRIP ice core (Barbante et al., 2013) the historically dated AD 79 eruption of Vesuvius has been used as a reference point in the GICC05 chronology (Vinther et al., 2006). However, our results indicate a timescale offset of -11 ± 6 years (2σ) at AD 79 (1871 years BP, see Fig. 10). Assuming that the tree-ring chronologies are correct at this time, this would imply an age of $\text{AD } 90 \pm 6$ for the GRIP tephra layer – incompatible with an attribution to the age of the Vesuvius eruption within 2σ . This result is in agreement with the analysis by Sigl et al. (2015) who recently counted annual layers in the NEEM and NEEM-2011-S1 ice cores and dated this marker horizon to AD 87 and 89, respectively.

The age of the Minoan eruption of Santorini has long been debated and the presence of an unequivocally attributable signal in the ice core records has been questioned (Pearce et al., 2004; Hammer et al., 1987, 2003; Friedrich et al., 2006). The GICC05 age of 3591 ± 5 BP of an identified tephra horizon is incompatible with the radiocarbon based age of 3563 ± 14 cal BP of the Santorini eruption ($\Delta = -28 \pm 15$ years). Our results indicate a chronology difference of -20 ± 5 years around this time, reconciling the two aforementioned ages (see Fig. 10, open diamond). Hence, at least from a chronological point of view, it cannot be ruled out that the ice core tephra may be ascribable to the Santorini eruption (Muscheler, 2009).

Synchronizing the Greenland ice core and radiocarbon timescales

F. Adolphi and
R. Muscheler

Title Page

Abstract

Introduction

Conclusions

References

Tables

Figures

◀

▶

◀

▶

Back

Close

Full Screen / Esc

Printer-friendly Version

Interactive Discussion

Volcanic glass shards from the Saksunarvatn ash have been found in the GRIP ice core (Grönvold et al., 1995), as well as in multiple marine, lacustrine and terrestrial sites, of which the Lake Kråkenes record provides the highest resolution radiocarbon based age for the deposit (Lohne et al., 2013). The dating difference of -86 ± 35 years between the radiocarbon based age by Lohne et al. (2013) ($10\,210 \pm 35$ calBP, $\pm 1\sigma$) and the GICC05 age (10 296 BP, Abbott and Davies, 2012) of the Saksunarvatn ash is consistent with our estimated timescale difference of -66 ± 10 years during this time interval.

In summary, our results are consistent within uncertainties with all independent age markers that link the GICC05 and IntCal13 timescales over the Holocene.

Figure 11 displays the inferred IntCal13-GICC05 timescale differences in comparison to the GICC05 maximum counting error (Rasmussen et al., 2006; Vinther et al., 2006). Assuming that the tree-ring chronologies underlying IntCal13 are accurate throughout the Holocene our results imply an underestimation of the absolute dating uncertainty of GICC05 for large parts of the Holocene. Furthermore, it can be seen that the counting error appears to be systematic, in that most uncertain years (counted as 0.5 ± 0.5 years, Rasmussen et al., 2006) have indeed not been true calendar years during the Holocene. Nevertheless, when comparing the rate of change of the inferred IntCal13-GICC05 timescale difference to the rate of change of the maximum counting error (i.e. the relative maximum counting error) it can be seen that – even though systematic – the identification of uncertain years in the ice core records is accurate. Except for the most recent 2000 years where (potentially erroneous) fix-points like the Vesuvius eruption are used to constrain GICC05 the relative layer counting uncertainty appears to be an accurate uncertainty estimate. This can be seen in Fig. 11 (lower panel) which indicates that the rate of change of the GICC05 maximum counting error is consistent within error with the rate of change of the IntCal13-GICC05 timescale difference prior to 2000 years BP. This is important to note as it generally supports the GICC05 layer counting methodology and uncertainty which forms the basis of GICC05 back to 60 000 years BP (Svensson et al., 2008) even though the systematic nature of

Synchronizing the Greenland ice core and radiocarbon timescales

F. Adolphi and
R. Muscheler

Title Page

Abstract

Introduction

Conclusions

References

Tables

Figures

◀

▶

◀

▶

Back

Close

Full Screen / Esc

Printer-friendly Version

Interactive Discussion

ice core dating-bias that affects large parts of the Holocene. Nevertheless, the identification of uncertain years in the ice core during the Holocene is otherwise generally accurate as expressed in the relative counting error (Fig. 11 lower panel). This is important to note as it, in principle, supports the layer counting method and uncertainty estimates also beyond the period investigated here. Furthermore, it should be noted that these conclusions are based on the assumption that the tree-ring time scale is accurate.

Independent of the accuracy of either of the two chronologies we provided a high-precision transfer-function between the radiocarbon and Greenland ice core timescales. This allows radiocarbon dated and ice core paleoclimate records to be compared at high chronological precision which will improve studies of leads and lags within the climate system throughout the Holocene (Bronk Ramsey et al., 2014). Furthermore, the methodology outlined here can be applied to link high-resolution ^{14}C records such as floating tree-ring chronologies to ice core time scales and thus, aid in testing and improving the glacial radiocarbon dating calibration curve.

Acknowledgements. The study was supported by the Swedish Research Council (VR) through a Linnaeus grant to Lund University (LUCCI). This work was supported by a grant from the Swedish Research Council (Dnr: 2013-8421). We thank Anders Svensson for providing GICC05 snow accumulation rates.

References

- Abbott, P. M. and Davies, S. M.: Volcanism and the Greenland ice-cores: the tephra record, *Earth-Sci. Rev.*, 115, 173–191, doi:10.1016/j.earscirev.2012.09.001, 2012.
- Adolphi, F., Güttler, D., Wacker, L., Skog, G., and Muscheler, R.: Intercomparison of ^{14}C dating of wood samples at Lund University and ETH-Zurich AMS facilities: extraction, graphitization, and measurement, *Radiocarbon*, 55, 391–400, 2013.
- Adolphi, F., Muscheler, R., Svensson, A., Aldahan, A., Possnert, G., Beer, J., Sjolte, J., Björck, S., Matthes, K., and Thiéblemont, R.: Persistent link between solar activity

Synchronizing the Greenland ice core and radiocarbon timescales

F. Adolphi and
R. Muscheler

Title Page

Abstract

Introduction

Conclusions

References

Tables

Figures

◀

▶

◀

▶

Back

Close

Full Screen / Esc

Printer-friendly Version

Interactive Discussion

and Greenland climate during the Last Glacial Maximum, *Nat. Geosci.*, 7, 662–666, doi:10.1038/ngeo2225, 2014.

Alley, R. B., Finkel, R. C., Nishiizumi, K., Anandakrishnan, S., Shuman, C. A., Mershon, G., Zielinski, G. A., and Mayewski, P. A.: Changes in continental and sea-salt atmospheric loadings in Central Greenland during the most recent deglaciation – model-based estimates, *J. Glaciol.*, 41, 503–514, 1995.

Andersen, K. K., Svensson, A., Johnsen, S. J., Rasmussen, S. O., Bigler, M., Röthlisberger, R., Ruth, U., Siggaard-Andersen, M.-L., Peder Steffensen, J., and Dahl-Jensen, D.: The Greenland Ice Core Chronology 2005, 15–42 ka. Part 1: constructing the time scale, *Quaternary Sci. Rev.*, 25, 3246–3257, doi:10.1016/j.quascirev.2006.08.002, 2006.

Barbante, C., Kehrwald, N. M., Marianelli, P., Vinther, B. M., Steffensen, J. P., Cozzi, G., Hammer, C. U., Clausen, H. B., and Siggaard-Andersen, M.-L.: Greenland ice core evidence of the 79 AD Vesuvius eruption, *Clim. Past*, 9, 1221–1232, doi:10.5194/cp-9-1221-2013, 2013.

Bard, E., Raisbeck, G. M., Yiou, F., and Jouzel, J.: Solar modulation of cosmogenic nuclide production over the last millennium: comparison between ^{14}C and ^{10}Be records, *Earth Planet. Sc. Lett.*, 150, 453–462, doi:10.1016/s0012-821x(97)00082-4, 1997.

Blockley, S. P. E., Lane, C. S., Hardiman, M., Rasmussen, S. O., Seierstad, I. K., Steffensen, J. P., Svensson, A., Lotter, A. F., Turney, C. S. M., and Bronk Ramsey, C.: Synchronisation of palaeoenvironmental records over the last 60,000 years, and an extended INTIMATE event stratigraphy to 48,000 b2k, *Quaternary Sci. Rev.*, 36, 2–10, doi:10.1016/j.quascirev.2011.09.017, 2012.

Blunier, T., Chappellaz, J., Schwander, J., Dällenbach, A., Stauffer, B., Stocker, T. F., Raynaud, D., Jouzel, J., Clausen, H. B., Hammer, C. U., and Johnsen, S. J.: Asynchrony of Antarctic and Greenland climate change during the last glacial period, *Nature*, 394, 739–743, doi:10.1038/29447, 1998.

Bronk Ramsey, C., van der Plicht, J., and Weninger, B.: “Wiggle matching” radiocarbon dates, *Radiocarbon*, 43, 381–390, 2001.

Bronk Ramsey, C., Albert, P., Blockley, S., Hardiman, M., Lane, C., Macleod, A., Matthews, I. P., Muscheler, R., Palmer, A., and Staff, R. A.: Integrating timescales with time-transfer functions: a practical approach for an INTIMATE database, *Quaternary Sci. Rev.*, 106, 67–80, doi:10.1016/j.quascirev.2014.05.028, 2014.

Buizert, C., Adrian, B., Ahn, J., Albert, M., Alley, R. B., Baggenstos, D., Bauska, T. K., Bay, R. C., Bencivengo, B. B., Bentley, C. R., Brook, E. J., Chellman, N. J., Clow, G. D., Cole-Dai, J.,

Synchronizing the Greenland ice core and radiocarbon timescales

F. Adolphi and
R. Muscheler

Title Page

Abstract

Introduction

Conclusions

References

Tables

Figures

◀

▶

◀

▶

Back

Close

Full Screen / Esc

Printer-friendly Version

Interactive Discussion

Conway, H., Cravens, E., Cuffey, K. M., Dunbar, N. W., Edwards, J. S., Fegyveresi, J. M., Ferris, D. G., Fitzpatrick, J. J., Fudge, T. J., Gibson, C. J., Gkinis, V., Goetz, J. J., Gregory, S., Hargreaves, G. M., Iverson, N., Johnson, J. A., Jones, T. R., Kalk, M. L., Kippenhan, M. J., Koffman, B. G., Kreutz, K., Kuhl, T. W., Lebar, D. A., Lee, J. E., Marcott, S. A., Markle, B. R., Maselli, O. J., McConnell, J. R., McGwire, K. C., Mitchell, L. E., Mortensen, N. B., Neff, P. D., Nishiizumi, K., Nunn, R. M., Orsi, A. J., Pasteris, D. R., Pedro, J. B., Pettit, E. C., Price, P. B., Priscu, J. C., Rhodes, R. H., Rosen, J. L., Schauer, A. J., Schoenemann, S. W., Sendelbach, P. J., Severinghaus, J. P., Shturmakov, A. J., Sigl, M., Slawny, K. R., Souney, J. M., Sowers, T. A., Spencer, M. K., Steig, E. J., Taylor, K. C., Twickler, M. S., Vaughn, B. H., Voigt, D. E., Waddington, E. D., Welten, K. C., Wendricks, A. W., White, J. W. C., Winstrup, M., Wong, G. J., and Woodruff, T. E.: Precise inter-polar phasing of abrupt climate change during the last ice age, *Nature*, 520, 661–665, doi:10.1038/nature14401, 2015.

Cauquoin, A.: Use of ^{10}Be to predict atmospheric ^{14}C variations during the Laschamp Excursion: high sensitivity to cosmogenic isotope production calculations, *Radiocarbon*, 56, 67–82, doi:10.2458/56.16478, 2014.

Delaygue, G. and Bard, E.: An Antarctic view of Beryllium-10 and solar activity for the past millennium, *Clim. Dynam.*, 36, 2201–2218, doi:10.1007/s00382-010-0795-1, 2010.

Field, C. V., Schmidt, G. A., Koch, D., and Salyk, C.: Modeling production and climate-related impacts on ^{10}Be concentration in ice cores, *J. Geophys. Res.*, 111, D15107, doi:10.1029/2005jd006410, 2006.

Finkel, R. C. and Nishiizumi, K.: Beryllium 10 concentrations in the Greenland Ice Sheet Project 2 ice core from 3–40 ka, *J. Geophys. Res.*, 102, 26699, doi:10.1029/97jc01282, 1997.

Friedrich, M., Remmele, S., Kromer, B., Hofmann, J., Spurk, M., Kaiser, K. F., Orcel, C., and Küppers, M.: The 12,460-year Hohenheim oak and pine tree-ring chronology from central Europe – a unique annual record for radiocarbon calibration and paleoenvironment reconstructions, *Radiocarbon*, 46, 1111–1122, 2004.

Friedrich, W. L., Kromer, B., Friedrich, M., Heinemeier, J., Pfeiffer, T., and Talamo, S.: Santorini eruption radiocarbon dated to 1627–1600 B.C., *Science*, 312, 548, doi:10.1126/science.1125087, 2006.

Grönvold, K., Óskarsson, N., Johnsen, S. J., Clausen, H. B., Hammer, C. U., Bond, G., and Bard, E.: Ash layers from Iceland in the Greenland GRIP ice core correlated with oceanic and land sediments, *Earth Planet. Sc. Lett.*, 135, 149–155, doi:10.1016/0012-821X(95)00145-3, 1995.

Synchronizing the Greenland ice core and radiocarbon timescales

F. Adolphi and
R. Muscheler

Title Page

Abstract

Introduction

Conclusions

References

Tables

Figures

◀

▶

◀

▶

Back

Close

Full Screen / Esc

Printer-friendly Version

Interactive Discussion

Güttler, D., Adolphi, F., Beer, J., Bleicher, N., Boswijk, G., Christl, M., Hogg, A., Palmer, J., Vockenhuber, C., Wacker, L., and Wunder, J.: Rapid increase in cosmogenic ^{14}C in AD 775 measured in New Zealand kauri trees indicates short-lived increase in ^{14}C production spanning both hemispheres, *Earth Planet. Sc. Lett.*, 411, 290–297, doi:10.1016/j.epsl.2014.11.048, 2015.

Hammer, C. U., Clausen, H. B., Friedrich, W. L., and Tauber, H.: The Minoan eruption of Santorini in Greece dated to 1645 BC?, *Nature*, 328, 517–519, 1987.

Hammer, C. U., Kurat, G., Hoppe, P., Grum, W., and Clausen, H. B.: Thera eruption date 1645 BC confirmed by new ice core data?, in: *Proceedings of the SCIEEM 2000 – EuroConference Haindorf*, May 2001, Haindorf, 87–93, 2003.

Heikkilä, U. and Smith, A. M.: Production rate and climate influences on the variability of ^{10}Be deposition simulated by ECHAM5-HAM: globally, in Greenland, and in Antarctica, *J. Geophys. Res.-Atmos.*, 118, 2506–2520, doi:10.1002/jgrd.50217, 2013.

Heikkilä, U., Beer, J., and Feichter, J.: Meridional transport and deposition of atmospheric ^{10}Be , *Atmos. Chem. Phys.*, 9, 515–527, doi:10.5194/acp-9-515-2009, 2009.

Heikkilä, U., Beer, J., Abreu, J. A., and Steinhilber, F.: On the atmospheric transport and deposition of the cosmogenic radionuclides (^{10}Be): a review, *Space Sci. Rev.*, 176, 321–332, doi:10.1007/s11214-011-9838-0, 2011.

Hogg, A. G., Turney, C. S., Palmer, J. G., Southon, J., Kromer, B., Ramsey, C. B., Boswijk, G., Fenwick, P., Noronha, A., and Staff, R.: The New Zealand kauri (*Agathis australis*) research project: a radiocarbon dating intercomparison of Younger Dryas wood and implications for IntCal13, *Radiocarbon*, 55, 2035–2048, 2013.

Johnsen, S. J., Dahl-Jensen, D., Dansgaard, W., and Gundestrup, N.: Greenland palaeotemperatures derived from GRIP bore hole temperature and ice core isotope profiles, *Tellus B*, 47, 624–629, doi:10.1034/j.1600-0889.47.issue5.9.x, 1995.

Köhler, P., Muscheler, R., and Fischer, H.: A model-based interpretation of low-frequency changes in the carbon cycle during the last 120,000 years and its implications for the reconstruction of atmospheric $\Delta^{14}\text{C}$, *Geochem. Geophys. Geosy.*, 7, Q11N06, doi:10.1029/2005GC001228, 2006.

Kovaltsov, G. A. and Usoskin, I. G.: A new 3D numerical model of cosmogenic nuclide ^{10}Be production in the atmosphere, *Earth Planet. Sc. Lett.*, 291, 182–188, doi:10.1016/j.epsl.2010.01.011, 2010.

Synchronizing the Greenland ice core and radiocarbon timescales

F. Adolphi and
R. Muscheler

Title Page

Abstract

Introduction

Conclusions

References

Tables

Figures

◀

▶

◀

▶

Back

Close

Full Screen / Esc

Printer-friendly Version

Interactive Discussion

Kovaltsov, G. A., Mishev, A., and Usoskin, I. G.: A new model of cosmogenic production of radiocarbon ^{14}C in the atmosphere, *Earth Planet. Sc. Lett.*, 337–338, 114–120, doi:10.1016/j.epsl.2012.05.036, 2012.

Lal, D. and Peters, B.: Cosmic ray produced radioactivity on the earth, in: *Kosmische Strahlung II/Cosmic Rays II*, *Handbuch der Physik*, edited by: Sitte, K., Springer, Berlin Heidelberg, Germany, 551–612, doi:10.1007/978-3-642-46079-1_7, 1967.

Lane, C. S., Brauer, A., Blockley, S. P. E., and Dulski, P.: Volcanic ash reveals time-transgressive abrupt climate change during the Younger Dryas, *Geology*, 41, 1251–1254, doi:10.1130/g34867.1, 2013.

Lohne, Ø. S., Mangerud, J. A. N., and Birks, H. H.: Precise ^{14}C ages of the Vedde and Sak-sunarvatn ashes and the Younger Dryas boundaries from western Norway and their comparison with the Greenland Ice Core (GICC05) chronology, *J. Quaternary Sci.*, 28, 490–500, doi:10.1002/jqs.2640, 2013.

Masarik, J. and Beer, J.: Simulation of particle fluxes and cosmogenic nuclide production in the Earth's atmosphere, *J. Geophys. Res.-Atmos.*, 104, 12099–12111, doi:10.1029/1998jd200091, 1999.

Masarik, J. and Beer, J.: An updated simulation of particle fluxes and cosmogenic nuclide production in the Earth's atmosphere, *J. Geophys. Res.*, 114, D11103, doi:10.1029/2008jd010557, 2009.

Mayewski, P. A., Meeker, L. D., Twickler, M. S., Whitlow, S., Yang, Q., Lyons, W. B., and Prentice, M.: Major features and forcing of high-latitude Northern Hemisphere atmospheric circulation using a 110,000-year-long glaciochemical series, *J. Geophys. Res.*, 102, 26345, doi:10.1029/96jc03365, 1997.

Mekhaldi, F., Muscheler, R., Adolphi, F., Aldahan, A., Beer, J., McConnell, J. R., Possnert, G., Sigl, M., Svensson, A., Synal, H. A., Welten, K. C., and Woodruff, T. E.: Multi-radionuclide evidence for the solar origin of the cosmic-ray events of AD 774/5 and AD 993/4, *Nature communications*, in review, 2015.

Miyake, F., Nagaya, K., Masuda, K., and Nakamura, T.: A signature of cosmic-ray increase in AD 774–775 from tree rings in Japan, *Nature*, 486, 240–242, doi:10.1038/nature11123, 2012.

Miyake, F., Masuda, K., and Nakamura, T.: Another rapid event in the carbon-14 content of tree rings, *Nature Communications*, 4, 1748, doi:10.1038/ncomms2783, 2013.

Synchronizing the Greenland ice core and radiocarbon timescales

F. Adolphi and
R. Muscheler

Title Page

Abstract

Introduction

Conclusions

References

Tables

Figures

◀

▶

◀

▶

Back

Close

Full Screen / Esc

Printer-friendly Version

Interactive Discussion

BC date for Minoan eruption of Santorini, *Geochem. Geophys. Geos.*, 5, Q03005, doi:10.1029/2003GC000672, 2004.

Pedro, J., van Ommen, T., Curran, M., Morgan, V., Smith, A., and McMorrow, A.: Evidence for climate modulation of the ^{10}Be solar activity proxy, *J. Geophys. Res.*, 111, D21105, doi:10.1029/2005jd006764, 2006.

Pedro, J. B., McConnell, J. R., van Ommen, T. D., Fink, D., Curran, M. A. J., Smith, A. M., Simon, K. J., Moy, A. D., and Das, S. B.: Solar and climate influences on ice core ^{10}Be records from Antarctica and Greenland during the neutron monitor era, *Earth Planet. Sc. Lett.*, 355–356, 174–186, doi:10.1016/j.epsl.2012.08.038, 2012.

Pilcher, J. R., Baillie, M. G. L., Schmidt, B., and Becker, B.: A 7,272-year tree-ring chronology for western Europe, *Nature*, 312, 150–152, 1984.

Raisbeck, G. M., Yiou, F., Fruneau, M., Loiseaux, J. M., Lieuvin, M., and Ravel, J. C.: Cosmogenic $^{10}\text{Be}/^7\text{Be}$ as a probe of atmospheric transport processes, *Geophys. Res. Lett.*, 8, 1015–1018, doi:10.1029/GL008i009p01015, 1981.

Rasmussen, S. O., Andersen, K. K., Svensson, A. M., Steffensen, J. P., Vinther, B. M., Clausen, H. B., Siggaard-Andersen, M. L., Johnsen, S. J., Larsen, L. B., Dahl-Jensen, D., Bigler, M., Röthlisberger, R., Fischer, H., Goto-Azuma, K., Hansson, M. E., and Ruth, U.: A new Greenland ice core chronology for the last glacial termination, *J. Geophys. Res.*, 111, D06102, doi:10.1029/2005jd006079, 2006.

Reimer, P. J., Bard, E., Bayliss, A., Beck, J. W., Blackwell, P. G., Bronk Ramsey, C., Buck, C. E., Cheng, H., Edwards, R. L., Friedrich, M., Grootes, P. M., Guilderson, T. P., Hafflidason, H., Hajdas, I., Hatté, C., Heaton, T. J., Hoffmann, D. L., Hogg, A. G., Hughen, K. A., Kaiser, K. F., Kromer, B., Manning, S. W., Niu, M., Reimer, R. W., Richards, D. A., Scott, E. M., Southon, J. R., Staff, R. A., Turney, C. S. M., and van der Plicht, J.: IntCal13 and Marine13 radiocarbon age calibration curves 0–50,000 years cal BP, *Radiocarbon*, 55, 1869–1887, doi:10.2458/azu_js_rc.55.16947, 2013.

Roth, R. and Joos, F.: A reconstruction of radiocarbon production and total solar irradiance from the Holocene ^{14}C and CO_2 records: implications of data and model uncertainties, *Clim. Past*, 9, 1879–1909, doi:10.5194/cp-9-1879-2013, 2013.

Seierstad, I. K., Abbott, P. M., Bigler, M., Blunier, T., Bourne, A. J., Brook, E., Buchardt, S. L., Buizert, C., Clausen, H. B., Cook, E., Dahl-Jensen, D., Davies, S. M., Guillevic, M., Johnsen, S. J., Pedersen, D. S., Popp, T. J., Rasmussen, S. O., Severinghaus, J. P., Svensson, A., and Vinther, B. M.: Consistently dated records from the Greenland

Synchronizing the Greenland ice core and radiocarbon timescales

F. Adolphi and
R. Muscheler

Title Page

Abstract

Introduction

Conclusions

References

Tables

Figures

◀

▶

◀

▶

Back

Close

Full Screen / Esc

Printer-friendly Version

Interactive Discussion

GRIP, GISP2 and NGRIP ice cores for the past 104 ka reveal regional millennial-scale $\delta^{18}\text{O}$ gradients with possible Heinrich event imprint, *Quaternary Sci. Rev.*, 106, 29–46, doi:10.1016/j.quascirev.2014.10.032, 2014.

Siegenthaler, U., Heimann, M., and Oeschger, H.: ^{14}C variations caused by changes in the global carbon cycle, *Radiocarbon*, 22, 177–191, 1980.

Sigl, M., Winstrup, M., McConnell, J. R., Welten, K. C., Plunkett, G., Ludlow, F., Buntgen, U., Caffee, M. W., Chellman, N. J., Dahl-Jensen, D., Fischer, H., Kipfstuhl, S., Kostick, C., Maselli, O. J., Mekhaldi, F., Mulvaney, R., Muscheler, R., Pasteris, D. R., Pilcher, J. R., Salzer, M., Schupbach, S., Steffensen, J. P., Vinther, B., and Woodruff, T. E.: Timing and climate forcing of volcanic eruptions for the past 2,500 years, *Nature*, in press, 2015.

Southon, J.: A first step to reconciling the GRIP and GISP2 ice-core chronologies, 0–14,500 yr B.P., *Quaternary Res.*, 57, 32–37, doi:10.1006/qres.2001.2295, 2002.

Spurk, M., Leuschner, H. H., Baillie, M. G. L., Briffa, K. R., and Friedrich, M.: Depositional frequency of German subfossil oaks: climatically and non-climatically induced fluctuations in the Holocene, *Holocene*, 12, 707–715, doi:10.1191/0959683602hl583rp, 2002.

Stuiver, M., Braziunas, T. F., Grootes, P. M., and Zielinski, G. A.: Is there evidence for solar forcing of climate in the GISP2 oxygen isotope record?, *Quaternary Res.*, 48, 259–266, doi:10.1006/qres.1997.1931, 1997.

Stuiver, M., Reimer, P. J., Bard, E., Beck, J. W., Burr, G. S., Hughen, K., Kromer, B., McCormac, F. G., Van der Plicht, J., and Spurk, M.: INTCAL98 radiocarbon age calibration, 24000–0 cal BP, *Radiocarbon*, 40, 1041–1083, 1998.

Svensson, A., Andersen, K. K., Bigler, M., Clausen, H. B., Dahl-Jensen, D., Davies, S. M., Johnsen, S. J., Muscheler, R., Parrenin, F., Rasmussen, S. O., Röthlisberger, R., Seierstad, I., Steffensen, J. P., and Vinther, B. M.: A 60 000 year Greenland stratigraphic ice core chronology, *Clim. Past*, 4, 47–57, doi:10.5194/cp-4-47-2008, 2008.

Vinther, B. M., Clausen, H. B., Johnsen, S. J., Rasmussen, S. O., Andersen, K. K., Buchardt, S. L., Dahl-Jensen, D., Seierstad, I. K., Siggaard-Andersen, M. L., Steffensen, J. P., Svensson, A., Olsen, J., and Heinemeier, J.: A synchronized dating of three Greenland ice cores throughout the Holocene, *J. Geophys. Res.*, 111, D13102, doi:10.1029/2005jd006921, 2006.

Vonmoos, M., Beer, J., and Muscheler, R.: Large variations in Holocene solar activity: constraints from ^{10}Be in the Greenland Ice Core Project ice core, *J. Geophys. Res.*, 111, A10105, doi:10.1029/2005ja011500, 2006.

Yiou, F., Raisbeck, G. M., Baumgartner, S., Beer, J., Hammer, C., Johnsen, S., Jouzel, J., Kubik, P. W., Lestringuez, J., Stiévenard, M., Suter, M., and Yiou, P.: Beryllium 10 in the Greenland Ice Core Project ice core at Summit, Greenland, J. Geophys. Res., 102, 26783, doi:10.1029/97jc01265, 1997.

CPD

11, 2933–2975, 2015

Synchronizing the Greenland ice core and radiocarbon timescales

F. Adolphi and
R. Muscheler

Title Page

Abstract

Introduction

Conclusions

References

Tables

Figures



Back

Close

Full Screen / Esc

Printer-friendly Version

Interactive Discussion



Synchronizing the Greenland ice core and radiocarbon timescales

F. Adolphi and
R. Muscheler

Table 1. Performed carbon cycle sensitivity experiments. All percentage values refer to the control simulation under pre-industrial conditions.

	Control	S1	S2	S3	S4
Air/Sea Exchange	100 %	150 %	50 %	100 %	100 %
Ocean ventilation	100 %	100 %	100 %	150 %	50 %

[Title Page](#)
[Abstract](#)
[Introduction](#)
[Conclusions](#)
[References](#)
[Tables](#)
[Figures](#)

[Back](#)
[Close](#)
[Full Screen / Esc](#)
[Printer-friendly Version](#)
[Interactive Discussion](#)

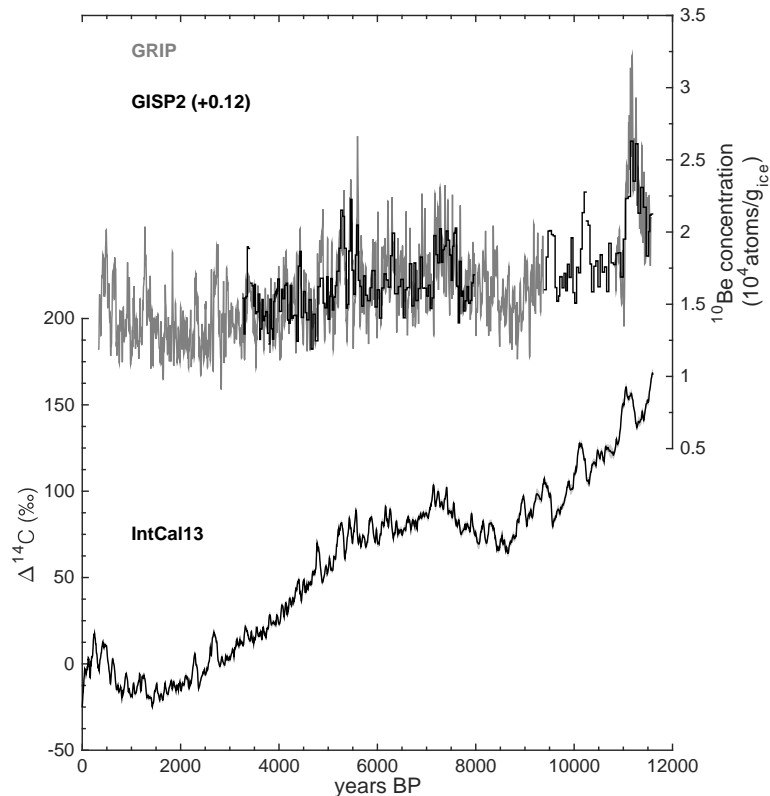



Figure 1. Key-data used in this study. Top: GRIP (grey, Vonmoos et al., 2006) and GISP2 (black, Finkel and Nishiizumi, 1997) Holocene ^{10}Be concentrations. The GRIP ^{10}Be record is smoothed by a 61 pt binomial filter (see Vonmoos et al., 2006). The GISP2 ^{10}Be record has been shifted by $+0.12 \times 10^4 \text{ atoms g}^{-1}$ to correct for a difference in the mean of the GRIP and GISP2 ^{10}Be records. Bottom: atmospheric $\Delta^{14}\text{C}$ as reconstructed from tree rings (Reimer et al., 2013 and references therein).

Synchronizing the Greenland ice core and radiocarbon timescales

F. Adolphi and
R. Muscheler

[Title Page](#)

[Abstract](#)

[Introduction](#)

[Conclusions](#)

[References](#)

[Tables](#)

[Figures](#)

[⏪](#)

[⏩](#)

[◀](#)

[▶](#)

[Back](#)

[Close](#)

[Full Screen / Esc](#)

[Printer-friendly Version](#)

[Interactive Discussion](#)

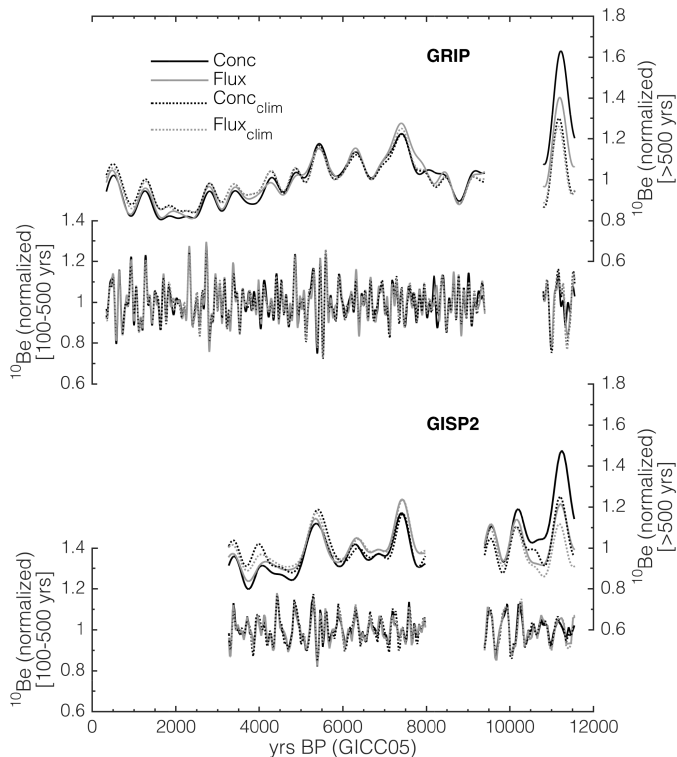


Figure 2. Comparison of ^{10}Be fluxes and concentrations over the Holocene. Solid black and grey curves denote ^{10}Be concentrations and fluxes, respectively. Dotted lines refer to the “climate corrected” (see text) versions of concentrations and fluxes with similar colour coding as solid lines. The top two panels show GRIP ^{10}Be for variations on time scales longer (top) than 500 years, and for wavelengths between 100–500 years (below). The 100 year cut-off has been applied for clarity of the figure. The agreement of the different ^{10}Be versions for shorter wavelengths is comparable to the 100–500 year band. The bottom two panels show GISP2 ^{10}Be for the same wavelengths as for GRIP.

Synchronizing the Greenland ice core and radiocarbon timescales

F. Adolphi and
R. Muscheler

Title Page

Abstract

Introduction

Conclusions

References

Tables

Figures

◀

▶

◀

▶

Back

Close

Full Screen / Esc

Printer-friendly Version

Interactive Discussion

Synchronizing the Greenland ice core and radiocarbon timescales

F. Adolphi and
R. Muscheler

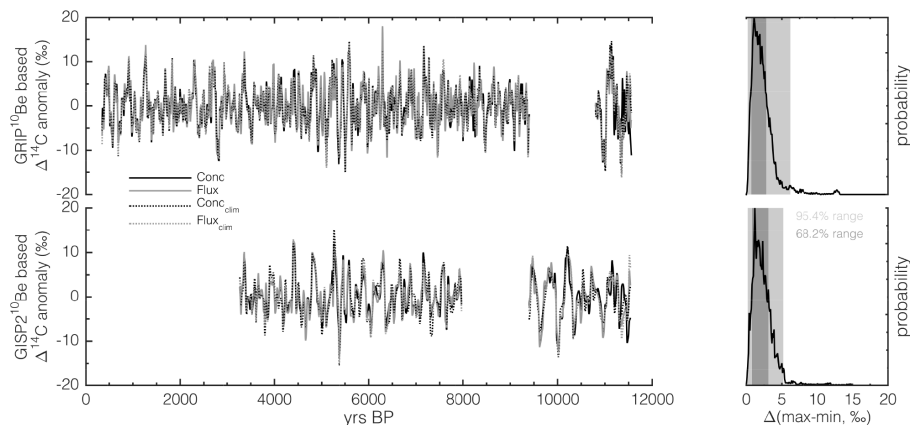


Figure 3. Centennial (< 500 years) $\Delta^{14}\text{C}$ variations modelled from GRIP (top) and GISP2 (bottom) ^{10}Be data. Left: modelled $\Delta^{14}\text{C}$ variations from ^{10}Be concentrations (solid black), fluxes (solid grey), “climate corrected” concentrations (dotted black), and “climate corrected” fluxes (dotted grey). Right: probability density functions for the maximum $\Delta^{14}\text{C}$ difference between curves shown on the left.

[Title Page](#)
[Abstract](#)
[Introduction](#)
[Conclusions](#)
[References](#)
[Tables](#)
[Figures](#)
[◀](#)
[▶](#)
[◀](#)
[▶](#)
[Back](#)
[Close](#)
[Full Screen / Esc](#)
[Printer-friendly Version](#)
[Interactive Discussion](#)

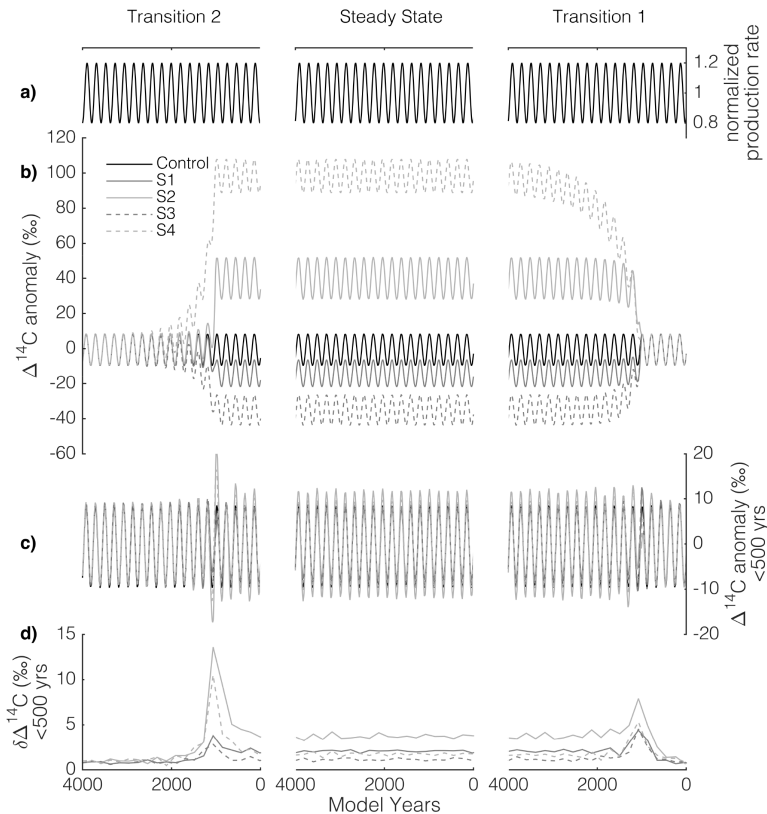


Figure 4. Carbon cycle sensitivity experiments. **(a)** Normalized ^{14}C production rate input to the model. **(b)** Modelled $\Delta^{14}\text{C}$ anomaly. **(c)** Centennial (< 500 year) anomalies of modelled $\Delta^{14}\text{C}$ shown in **(b)**. **(d)** Differences in the centennial $\Delta^{14}\text{C}$ variations **(c)** from the control run. All model runs and panels are shown for the transition from preindustrial to perturbed conditions (transition 1, right), steady state of the perturbed conditions (steady state, middle), and the transition back to preindustrial carbon cycle conditions (transition 2, left). See also Sect. 2.4.1.

Synchronizing the Greenland ice core and radiocarbon timescales

F. Adolphi and
R. Muscheler

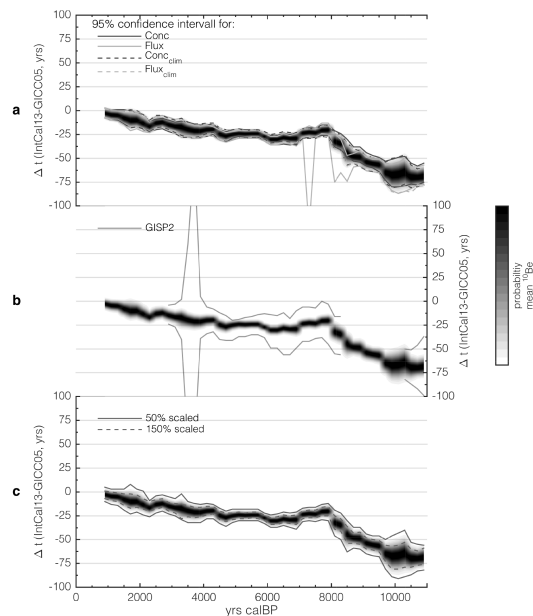


Figure 5. Probability distributions for IntCal13-GICC05 time differences distribution ($P_{s_{\text{scaled}}}(t_s)$, see Sect. 2.1) for each 1000 year window based on the mean of GRIP ^{10}Be concentrations, fluxes, and their climate corrected versions (grey-scale patches in all panels). The gap in the GRIP ^{10}Be record between 9400 and 10 800 BP has been filled with data from the GISP2 ice core. Each probability distribution is centred on the mean age of the investigated window. **(a)** Comparison between 95 % probability intervals based on GRIP ^{10}Be concentrations (solid dark grey line), fluxes (solid light grey line) and their “climate corrected” versions (dashed lines of corresponding colour). **(b)** Comparison between 95 % confidence intervals based on the mean of GISP2 ^{10}Be concentrations, fluxes, and their climate corrected versions. Results for GISP2 are only shown for periods where it has not been used to fill the gap in the GRIP record. **(c)** Comparison to results based on a different scaling (factors of 0.5 and 1.5 shown as solid and dashed lines, respectively) of the GRIP ^{10}Be record.

[Title Page](#)
[Abstract](#)
[Introduction](#)
[Conclusions](#)
[References](#)
[Tables](#)
[Figures](#)
[◀](#)
[▶](#)
[◀](#)
[▶](#)
[Back](#)
[Close](#)
[Full Screen / Esc](#)
[Printer-friendly Version](#)
[Interactive Discussion](#)

Synchronizing the Greenland ice core and radiocarbon timescales

F. Adolphi and
R. Muscheler

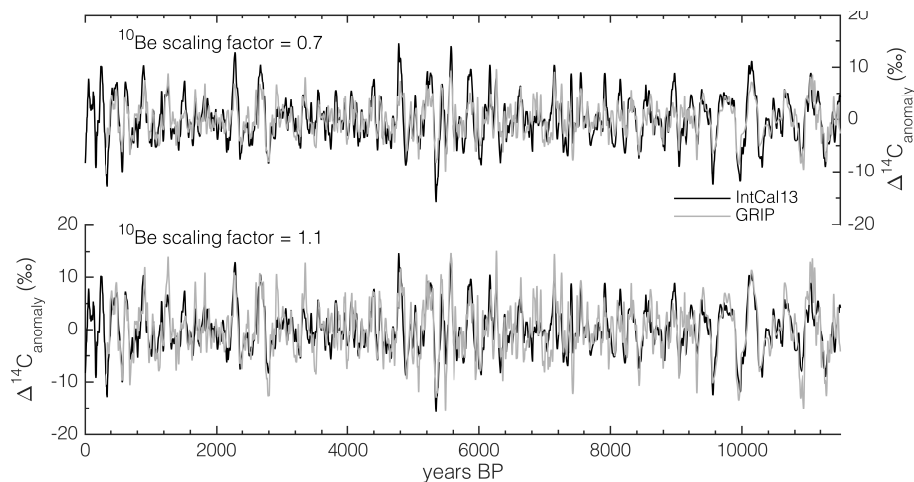


Figure 7. Comparison of synchronized tree-ring (black) and ice core (grey) based $\Delta^{14}\text{C}$ anomalies for $^{14}\text{C} : ^{10}\text{Be}$ ratios of 0.7 (top) and 1.1 (bottom).

[Title Page](#)[Abstract](#)[Introduction](#)[Conclusions](#)[References](#)[Tables](#)[Figures](#)[◀](#)[▶](#)[◀](#)[▶](#)[Back](#)[Close](#)[Full Screen / Esc](#)[Printer-friendly Version](#)[Interactive Discussion](#)

Synchronizing the Greenland ice core and radiocarbon timescales

F. Adolphi and
R. Muscheler

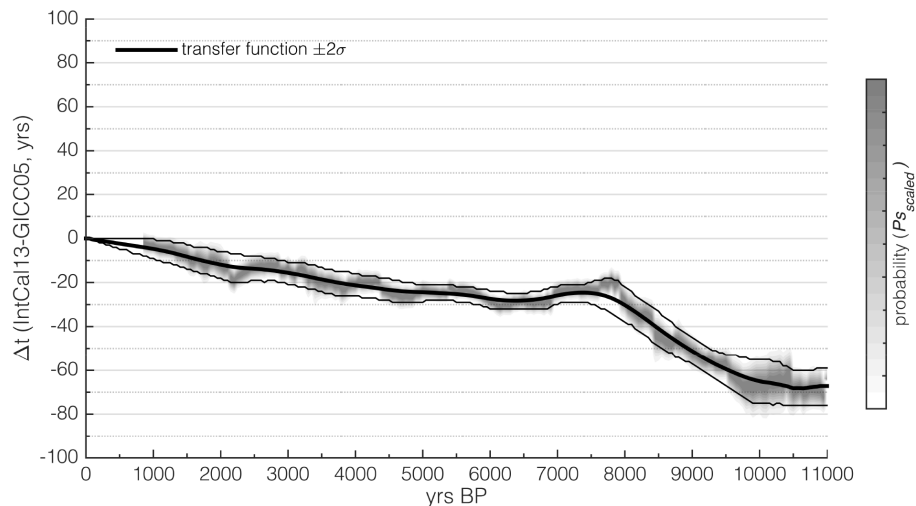


Figure 9. IntCal13-GICC05 age transfer function (black lines) based on the probability distributions ($P_{s_{scaled}}(t_s)$, grey shading) obtained from comparing the GRIP ^{10}Be -based $\Delta^{14}\text{C}$ (mean of concentration, flux and climate corrections) and IntCal13 $\Delta^{14}\text{C}$ records.

Title Page

Abstract

Introduction

Conclusions

References

Tables

Figures

◀

▶

◀

▶

Back

Close

Full Screen / Esc

Printer-friendly Version

Interactive Discussion



Synchronizing the Greenland ice core and radiocarbon timescales

F. Adolphi and
R. Muscheler

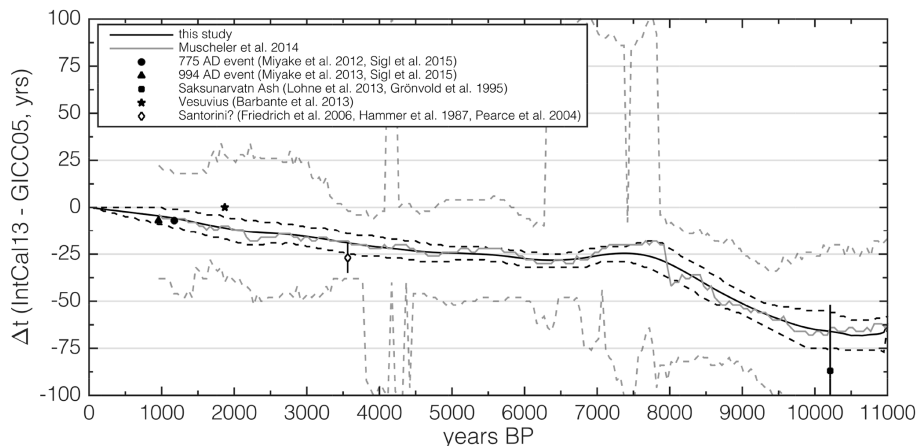


Figure 10. Comparison of the derived IntCal13-GICC05 timescale transfer-function (black lines, this study), the results by Muscheler et al. (2014, grey lines), and independent age markers that have been linked independently to both the IntCal13 and GICC05 timescales at high precision (symbols). The results of this study and Muscheler et al. are shown with their respective 95% confidence intervals (dashed lines). The independent age markers are plotted as the difference between their estimated ages based on radiocarbon dating (Saksunarvatn Ash, Santorini), historical documents (Vesuvius) and dendrochronology (775 and 994 AD events), and their respective GICC05-ages. The plotted 1σ error bars largely reflect uncertainties in the radiocarbon-dating and calibration of the Saksunarvatn Ash (Lohne et al., 2013) and the Santorini eruption (Friedrich et al., 2006). Note that the identification of the Santorini tephra in ice cores has been challenged based on its geochemistry (Pearce et al., 2004).

[Title Page](#)
[Abstract](#)
[Introduction](#)
[Conclusions](#)
[References](#)
[Tables](#)
[Figures](#)
[◀](#)
[▶](#)
[◀](#)
[▶](#)
[Back](#)
[Close](#)
[Full Screen / Esc](#)
[Printer-friendly Version](#)
[Interactive Discussion](#)

Synchronizing the Greenland ice core and radiocarbon timescales

F. Adolphi and
R. Muscheler

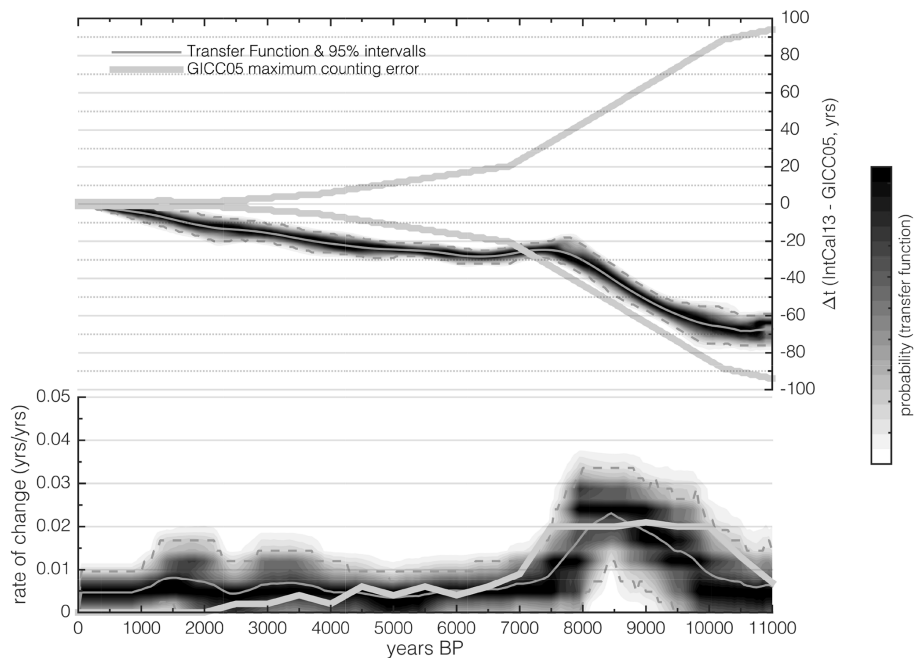


Figure 11. Top: comparison of the derived IntCal13-GICC05 transfer function (thin grey lines and shading, dashed lines denote the 95 % confidence interval) and the GICC05 maximum counting error (bold grey lines). Bottom: same as above but expressed as the rate of change (years^{years}⁻¹) of the GICC05 maximum counting error and the derived timescale transfer-function.